

Shifting and broadening in the fundamental band of CO highly diluted in He and Ar: A comparison with theory

Caiyan Luo, R. Wehr, J. R. Drummond, A. D. May, F. Thibault, J. Boisssoles, J. M. Launay, C. Boulet, J.-P. Bouanich, and J.-M. Hartmann

Citation: *The Journal of Chemical Physics* **115**, 2198 (2001); doi: 10.1063/1.1383049

View online: <http://dx.doi.org/10.1063/1.1383049>

View Table of Contents: <http://scitation.aip.org/content/aip/journal/jcp/115/5?ver=pdfcov>

Published by the [AIP Publishing](#)

Articles you may be interested in

[Pressure broadening, shift and asymmetry of the 326.1 nm Cd line perturbed by N₂ and CH₄](#)
AIP Conf. Proc. **645**, 188 (2002); 10.1063/1.1525453

[Comparison of an ab initio calculation of the CO-Ar P\(2\) line shape with high-resolution measurements](#)
AIP Conf. Proc. **645**, 161 (2002); 10.1063/1.1525448

[Semiclassical modeling of infrared pressure-broadened linewidths: A comparative analysis in CO₂ – Ar at various temperatures](#)
J. Chem. Phys. **115**, 7436 (2001); 10.1063/1.1394941

[Broadening, shifting, and line asymmetries in the 2–0 band of CO and CO – N₂: Experimental results and theoretical calculations](#)
J. Chem. Phys. **113**, 158 (2000); 10.1063/1.481783

[Quantum scattering calculations for H₂S–He between 1–600 K in comparison with pressure broadening, shift, and time resolved double resonance experiments](#)
J. Chem. Phys. **111**, 8893 (1999); 10.1063/1.480234



NEW Special Topic Sections

NOW ONLINE
Lithium Niobate Properties and Applications:
Reviews of Emerging Trends

AIP | Applied Physics
Reviews

Shifting and broadening in the fundamental band of CO highly diluted in He and Ar: A comparison with theory

Caiyan Luo, R. Wehr, J. R. Drummond, and A. D. May^{a)}
Department of Physics, University of Toronto, Toronto, M5S 1A7 Canada

F. Thibault, J. Boisssoles, and J. M. Launay
Laboratoire PALMS (UMR-CNRS) Université Rennes I, Campus de Beaulieu, 35042, France

C. Boulet, J.-P. Bouanich, and J.-M. Hartmann
Laboratoire de Photophysique Moléculaire (CNRS) Université Paris Sud. Bât 350, Campus d'Orsay, 91405 Orsay CEDEX, France

(Received 10 January 2001; accepted 11 May 2001)

We present measurements of the shifts and widths of the rovibrational lines of the fundamental band of CO highly diluted in He and Ar at 296 K. The shifts are decomposed into parts odd and even in the line number, m . These are then compared with close coupled calculations carried out with the best known interaction potentials. There is general agreement between the calculated and measured values of the broadening and shifting. Furthermore, the results illustrate that the decomposition of the shifts into parts, odd and even in m , is a powerful tool for separating out the relative contributions of the isotropic and anisotropic part of the interaction to the shifts and which part needs to be corrected if there is a discrepancy. Thus, shift measurements can be added to the list of experiments that may be used to determine reliable interaction potentials. The results also show, given a potential, that close coupled calculations are accurate and could be used to confirm or establish empirical models of the temperature dependence of the broadening or shifting, etc. Such modeling is important at atmospheric physics. © 2001 American Institute of Physics.
[DOI: 10.1063/1.1383049]

I. INTRODUCTION

There are several reasons for the recent increased interest in spectral line shapes. One is the number of observations that are at variance with the conventional speed-independent line-shape models (Lorentzian or Voigt). These deviations are now being detected due to the ever increasing precision and sensitivity associated with laser-based spectrometers and pose a theoretical challenge as to their detailed explanation. Another reason is the need to model the line shapes for the expanding number of studies of remote sensing of atmospheric constituents. We are concerned with this second area, where the main problem arises from the need to know the absorption profile for a large number of lines for a range of temperature, pressure, and mixture ratios. Departures from simple line-shape models brought on by speed-dependent effects are generally less important under atmospheric conditions. They may become more important in the future as the precision of atmospheric measurements increases.

At this point in time, it might be argued, for molecules of atmospheric interest, that quantal calculations with reasonable but known intermolecular potentials are accurate enough to calculate the widths and shifts of lines, the parameters required for the spectral profile of isolated lines. This argument fails on two counts. First, the potential may not be known or at least in part require a knowledge of the shift or width before it can be determined and second, the sheer size

of the problem precludes all but a very limited number of quantal calculations. A practical way around these difficulties is to model the temperature, pressure, and compositional dependence of the broadening and shifting (and mixing if required) and to justify the model by a combination of laboratory experiments and quantal calculations for a few test cases. We subscribe to this approach and in this paper focus on the justification process, i.e., the use of quantal calculations and experimental results to verify or confirm the potential used in the calculations. Once this has been done for a given composition or perturber, then a few calculations at different temperatures can be performed to justify any empirical temperature dependence of the broadening (cf. Refs. 1 and 2) and shifting, etc.

For illustrative purposes we examine the case of the fundamental rovibrational band of CO perturbed by He or Ar. For He, at least, we believed that the interaction potential was well known. In the experimental section we report new measurements of the shifts for many P and R branch lines of the fundamental band. Less emphasis is placed on measurements of the widths as these were given previously, albeit at a slightly higher temperature.³ In the theoretical section we present the results of close coupled quantal calculations followed by a comparison with the experimental data. For the shifts, we follow the pioneering work of Herman⁴ by comparing the calculated and measured shifts by first decomposing them into a part symmetric or even in m and a part antisymmetric or odd in m ($m = -J$ for the P branch and $m = J + 1$ for the R branch). As shown by Herman (using a

^{a)}Electronic mail: dmay@physics.utoronto.ca

second-order semiclassical theory) this helps to disentangle the effect on the shifts of the isotropic and anisotropic part of the potential. As we shall see below, if there is a disagreement between theory and experiment, such a decomposition aids in identifying which part of the potential needs to be revised. Using any one of a number of semiclassical calculations would fail to resolve such a discrepancy, as there would always be an additional doubt as to the accuracy of the theory itself.⁵ On the other hand, full close coupled quantum calculations are, themselves, generally considered to be accurate to about the 1% level for a given potential.

II. EXPERIMENTAL DETAILS

The basic apparatus consists of a difference frequency spectrometer and a conventional two-beam absorption experiment. The spectrometer has previously been described by Duggan *et al.*⁶ To this was added a detector and a second absorption cell containing CO at low pressure. Both absorption spectra were recorded simultaneously, point by point. The second cell provides a frequency marker located essentially at the frequency of the free molecule, for each of the lines studied in the fundamental band. The temperature of the sample cell was 296 ± 1 K. Two sets of measurements were made, one with CO highly diluted in He and the other with CO highly diluted in Ar. For further experimental details and an example of simultaneously recorded spectra, the reader is referred to Luo *et al.*⁷

As in Ref. 7, the center of the reference line was determined by fitting it to a Lorentzian profile. For the sample under study, the lines were first decomposed into a Lorentzian profile and an associated dispersion or asymmetric profile. The latter accounts, in principle, for the presence of weak line mixing.^{8,9} It is the center of the strong symmetric component that is used to determine a frequency shift. This is equivalent to the frequency shift of the “center of gravity” of the line. In practice, because the amplitude of the asymmetric component is very small, the shifts reported are the same (within experimental error) as the shifts of the peak of the lines. The widths (HWHM) were determined from the

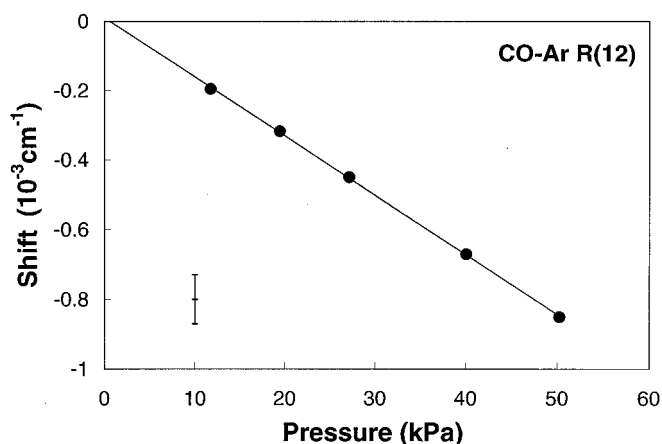


FIG. 1. Shift of the R(12) line of CO–Ar as a function of pressure. The points are the mean of several measurements. The error bar shown is the 1σ value for a single measurement made at 50 kPa.

TABLE I. Shifting coefficients for CO–He at 296 K in units of $10^{-3} \text{ cm}^{-1} \text{ atm}^{-1}$. Estimated error bars (1σ) $\pm 0.7 \times 10^{-4} \text{ cm}^{-1} \text{ atm}^{-1}$.

$ m $	P branch	R branch
17	-0.68	+0.35
15	-0.73	+0.32
13	-0.75	+0.36
11	-0.72	+0.24
9	-0.58	+0.28
7	-0.40	+0.21
6	-0.41	+0.13
4	-0.33	-0.04
3	-0.26	-0.18
2	-0.21	-0.15
1	-0.15	-0.19

Lorentzian fit to the symmetric component of each line. These too are essentially unaffected (within experimental error) by the presence of weak mixing.

Figure 1 shows a plot of the shift of the R(12) line of CO in Ar as a function of pressure. The fitted straight line passes through the origin within experimental error (± 2 MHz). Being proportional to pressure establishes, at least as far as the shifts are concerned, that speed-dependent effects^{10,11} may be neglected. We are therefore justified in measuring the shifting coefficient (slope of the line in Fig. 1) for all other lines by recording the shift at a single pressure of about 50 kPa and dividing by the pressure. The same procedure was used to determine the broadening coefficients.

III. SHIFTING COEFFICIENTS (EXPERIMENTAL)

Shifting coefficients for many P and R branch lines are given in Tables I and II. The 1σ error limits quoted were determined from repeated measurements of individual lines. (See below about the reproducibility of the measurements.) Figures 2(a) and 2(b) compare the present measurements with previous “room temperature” measurements of the shifts.^{12–16} We see from Fig. 2(a) that the absolute value of

TABLE II. Shifting coefficients for CO–Ar at 296 K in units of $10^{-3} \text{ cm}^{-1} \text{ atm}^{-1}$. Estimated error bars (1σ) $\pm 1.5 \times 10^{-4} \text{ cm}^{-1} \text{ atm}^{-1}$.

$ m $	P branch	R branch
24		-2.95
21	-3.33	-2.69
19	-3.35	-2.30
17	-3.41	-2.04
16	-3.43	-1.91
15	-3.33	-1.85
14	-3.41	
13	-3.38	-1.72
11	-3.32	-1.70
9	-3.26	-1.42
8	-3.24	-1.37
7	-3.37	-1.28
6	-3.24	
5	-3.02	-1.28
4	-2.72	-1.21
3	-2.21	-1.26
2	-1.39	-1.53
1	-1.32	-1.28

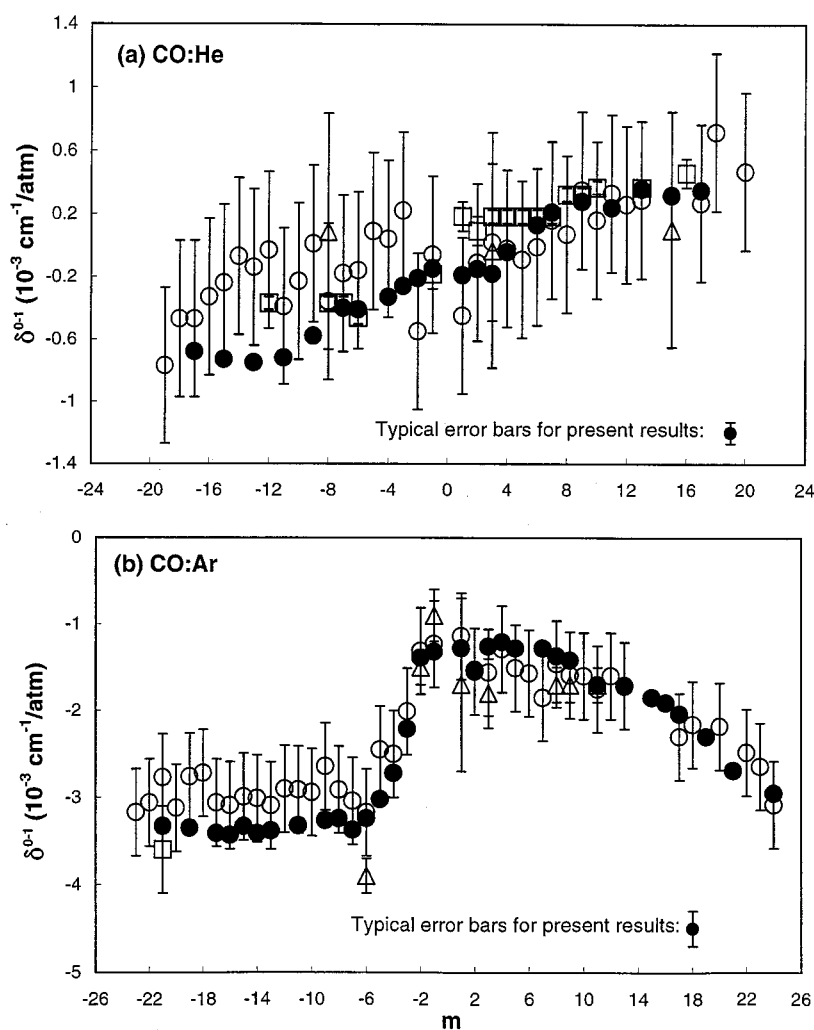


FIG. 2. A comparison of previous measurements of shifting coefficients near room temperature with the present results (solid points); (a) CO-He; open circles (Ref. 14), open squares (Ref. 13), open triangles (Ref. 12); (b) CO-Ar; open circles (Ref. 14), open triangles (Ref. 15), open squares (Ref. 16).

the shifting coefficients in CO-He is very small, being less than $1 \times 10^{-3} \text{ cm}^{-1}/\text{atm}$ for all lines measured. All of the measurements are generally consistent but ours are typically a factor of 5 more precise than those given in Refs. 12 and 14. There is disagreement between our results for the R(1)-R(4) line and the measurements of Thibault *et al.*¹³ (open squares). We note that there are two sets of results reported in Ref. 13 for the first overtone and these often differ by more than the estimated error limits. This represents some experimental basis for preferring the present results over those of Ref. 13 for the four R, low m , lines of the fundamental band of CO-He.

The shifting coefficients in CO-Ar [Fig. 2(b)] are more negative than in CO-He, reaching values on the order of $-4 \times 10^{-3} \text{ cm}^{-1}/\text{atm}$ in the P branch. Again we see, generally speaking, that all of the measurements are consistent within quoted error limits. The present results are about a factor of 3 more precise than the older measurements¹⁴ and have a precision comparable to the few measurements reported in Refs. 15 and 16. There may be systematic differences between the experiments as they were not all performed at exactly the same temperature. There is limited information available about the temperature dependence of the shifts,¹⁷ but the differences are probably small given the

small range of temperature over which the various experiments were carried out.

In Figs. 3(a) and 4(a) we present our results alone. In Figs. 3(b) and 4(b) we plot δ_e^{0-1} the part of the shifts that is even in m , where δ_e^{0-1} is defined by $\delta_e^{0-1}(m) = (1/2) \times [\delta^{0-1}(m) + \delta^{0-1}(-m)]$. For m positive (negative) $\delta^{0-1}(m)$ stands for the shift in an R (P) line of the fundamental band. In Figs. 3(c) and 4(c) we plot δ_o^{0-1} , the part of the shifts that is odd in m , where δ_o^{0-1} is defined by $\delta_o^{0-1}(m) = (1/2) [\delta^{0-1}(m) - \delta^{0-1}(-m)]$. This is the decomposition suggested by Herman⁴ and which we propose to use as a tool to aid in identifying the source of any error in the potential, should there be a disagreement between accurate quantal calculations and the measurements. The solid lines in Figs. 3(a), 3(b), 3(c), and Fig. 4(c) join the theoretical points, which we explain below.

First, however, we address the question of the reproducibility of our shift measurements. As a test of the reproducibility we reconfigured the difference frequency spectrometer, the ancillary optics and absorption cells, and with independent researchers repeated the measurements of the shifts for five of the lines in CO-Ar, all at a single pressure of 86 kPa. The new points are shown as open squares in Fig.

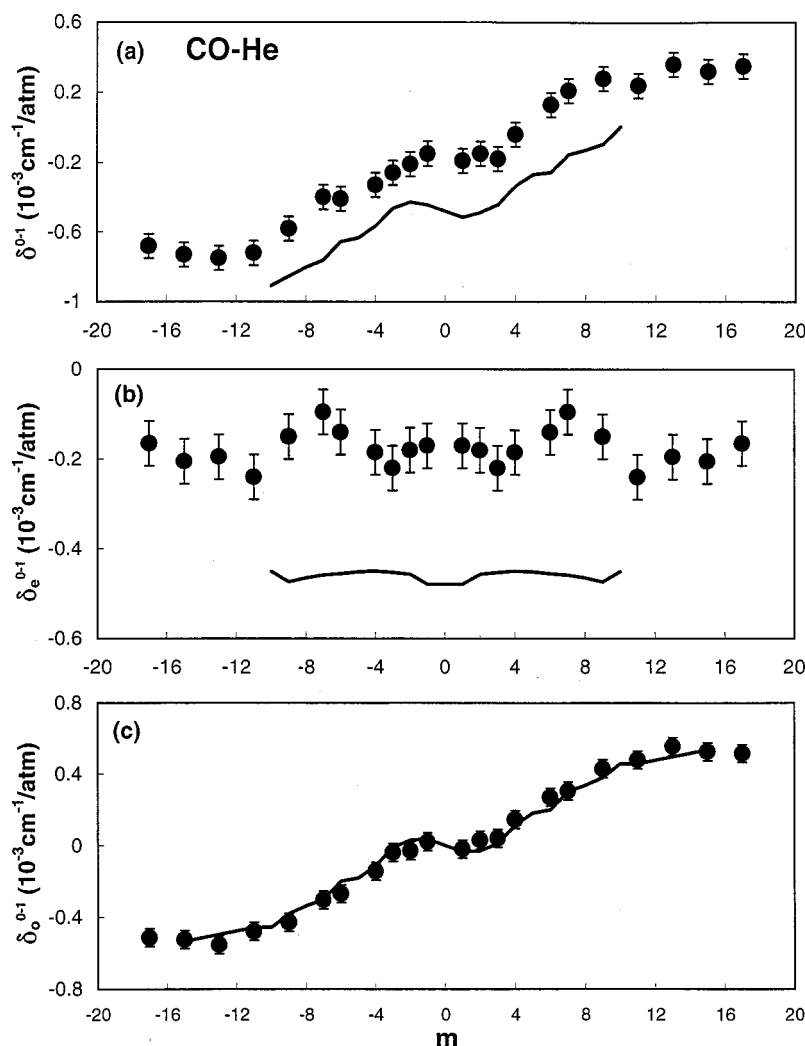


FIG. 3. Panel (a), the points are the measured shifting coefficient in CO–He at 296 K as a function of m . In panels (b) and (c) these are decomposed into a part even in m and a part odd in m . The broken lines join the calculated values.

4. The results indicate that our measurements are very reliable but perhaps a more realistic estimate of the 1σ error bar would be about $0.2 \times 10^{-3} \text{ cm}^{-1}/\text{atm}$ for most of the lines. For the low m lines the error will be higher since these lines are much broader [see Fig. 5(b) below] and thus more difficult to measure. It is the average error bar of $0.2 \times 10^{-3} \text{ cm}^{-1}$ that is shown in Fig. 4(a). The corresponding average error bars for Figs. 4(b) and 4(c) are thus $0.14 \times 10^{-3} \text{ cm}^{-1}$.

IV. BROADENING COEFFICIENTS (EXPERIMENTAL)

The measured broadening coefficients (HWHM/atm) are listed in Tables III and IV and plotted in Figs. 5(a) and 5(b). Upon examination of the tables, we see that the corresponding P and R branch lines have the same coefficient to almost three significant figures. In Ref. 3 we compared our room temperature results with earlier measurements. Here, we note that the new measurements for both CO–He and CO–Ar (filled circles) are consistent with our earlier measurements³ at 301.5 K (open circles), provided the broadening coefficients, γ , satisfy the accepted scaling law, γT^N equal to a constant, with N set at a typical value of 0.7.² Nevertheless, we consider the earlier results to be the more reliable as more

attention was paid in Ref. 3 to those experimental details that influence the width (but not the frequency) measurements. Note the very expanded vertical scale in Fig. 5(a). The broadening in CO–He only varies by 10% with changing line number. In CO–Ar, the variation with varying m is by a factor of 2. In Fig. 5, the solid lines connect the theoretical values, which we now explain.

V. THEORY

Neglecting speed-dependent effects and using the impact approximation for isolated lines, the line-shape function for a spectral line, $(v_i, j_i \rightarrow v_f, j_f)$, is Lorentzian⁹ with a width and shift given by the real and imaginary parts, respectively, of a thermally averaged cross section $\sigma_{fi}^{(1)}$ according to

$$\gamma_{fi} - i\delta_{fi} = \frac{n_p \langle v \rangle}{2\pi c} \int_0^\infty x e^x \sigma_{fi}^{(1)}(x) dx, \quad (1)$$

where $x = E_k/k_B T$ is the normalized relative kinetic energy, $\langle v \rangle$ the mean relative speed, n_p the number density of the perturbers, T the temperature and k_B Boltzmann's constant. In the close coupling theory of Fano and Ben Reuven, the cross section^{18,19} is given by a sum over scattering matrices, as follows:

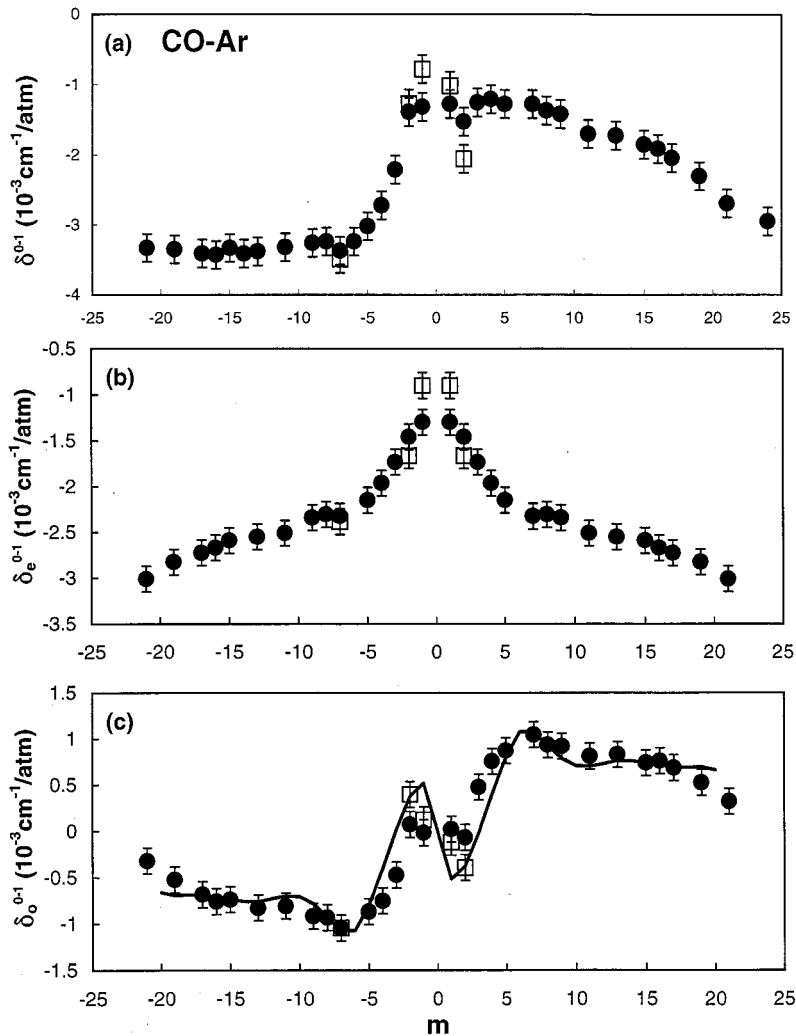


FIG. 4. Panel (a), the point are the measured shifting coefficient in CO–Ar at 296 K as a function of m . The open squares are recent independent measurements of the shifting coefficients of several lines. In panels (b) and (c) the results are decomposed into a part even in m and a part odd in m . The broken line joins the calculated values. The open squares are our recent independent remeasurements of the shifts for a few sample lines.

$$\begin{aligned} \sigma_{fi}^{(1)} = & \frac{\pi}{k^2} \sum_{J_i J_f} \sum_{l l'} (2J_i + 1)(2J_f + 1) \\ & \times (-1)^{l-l'} \begin{Bmatrix} J_i & 1 & J_f \\ J_f & l & J_i \end{Bmatrix} \begin{Bmatrix} J_i & 1 & J_f \\ J_f & l' & J_i \end{Bmatrix} \\ & \times [\delta_{ll'} - \langle v_{ij_i l'} | S^{J_i}(E_k + E_{j_i}) | v_{ij_i j_i} \rangle \\ & \times \langle v_{j_f j_f l'} | S^{J_f}(E_k + E_{j_f}) | v_{j_f j_f l'} \rangle^*], \end{aligned} \quad (2)$$

Here, J is the total angular momentum, l the partial wave collisional angular momentum, k the collisional wave number, and primes indicate postcollisional values. The various momenta are combined through the $6j$ symbols, $\{\}$.

The S matrices required for Eq. (2) are obtained by solving a standard scattering problem. The most widely used program for this purpose is the MOLSCAT code of Hutson and Green,²⁰ which employs a space-fixed coordinate frame.²¹ In the present work we use MOLCOL,²² a computer code which uses a coordinate system fixed at the center of mass of a colliding pair with the z axis chosen as the line joining the centers of mass of the projectile and target.²³ Here, the pressure broadening cross sections are related to the irreducible components of the S matrix^{24–26} through the equation

$$\begin{aligned} \sigma_{fi}^{(1)}(x) = & \frac{\pi}{k^2} \sum_{\lambda} (-1)^{\lambda} \begin{Bmatrix} J_i & J_i & \lambda \\ J_f & J_f & 1 \end{Bmatrix} \\ & \times \sum_{l l'} [(2l + 1) \sqrt{(2j_i + 1)2j_f + 1}] \delta_{ll'} \delta_{\lambda 0} \\ & - \langle v_{ij_i l'} | S^{\lambda}(E_k + E_{j_i}) | v_{ij_i l'} \rangle \\ & \times \langle v_{j_f j_f l'} | S^{\lambda}(E_k + E_{j_f}) | v_{j_f j_f l'} \rangle^*], \end{aligned} \quad (3)$$

where $\lambda = \mathbf{l} - \mathbf{l}'$ is now the angular momentum transferred during the collision. Coupling between different vibrational manifolds is much smaller than coupling among rotational levels within a given vibrational level and is neglected in Eq. (3), i.e., we neglect the contribution of vibrationally inelastic collisions. Thus, the scattering equations become block diagonal in v and may be solved separately for each vibrational level. The Johnson log derivative propagator²⁷ was used to solve the equations. The propagation was carried out from a minimum distance of 2.75 bohr to a maximum distance of 30 bohr for CO–He and from 4 to 35 bohr for CO–Ar with a constant step size corresponding to 8 points per half wavelength for the open channel of highest kinetic energy (in the

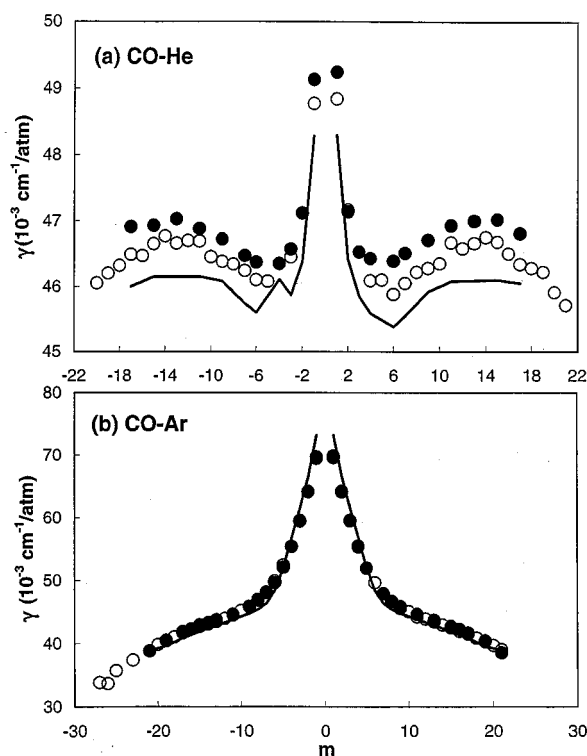


FIG. 5. Panel (a), solid points, broadening coefficients in CO–He at 296 K. The open circles are previously measured values at 301.5 K (Ref. 3). The broken line joins the theoretical values. Panel (b), as in (a) except the results are for CO–Ar.

asymptotic limit). All energetically open rotational levels of CO and at least three (for He) or five (for Ar) closed channels were included at each total energy. No limits were set for the orbital (l) and total (J) angular momentum numbers. The sum over partial waves in Eq. (3) was extended to obtain converged cross sections to 1% or better. For example, more than 200 partial waves were taken into account for CO–Ar at a total energy of 377 K.

For CO–He, calculations were performed in the ground vibrational state for a grid of 33 total energies from 5 to 1000 K. Then, a similar grid was generated for the upper vibrational level. The thermal average in Eq. (1) was carried out using common routines. For CO–Ar, calculations were made

TABLE III. Broadening coefficients for CO–He at 296 K in units of $10^{-3} \text{ cm}^{-1} \text{ atm}^{-1}$. Estimated error bars (1σ) $\pm 0.5 \times 10^{-4} \text{ cm}^{-1} \text{ atm}^{-1}$.

$ m $	P branch	R branch
17	46.91	46.81
15	46.93	47.02
13	47.03	47.00
11	46.88	46.93
9	46.72	46.71
7	46.47	46.51
6	46.37	46.39
4	46.35	46.43
3	46.57	46.53
2	47.12	47.14
1	49.13	49.24

TABLE IV. Broadening coefficients for CO–Ar at 296 K in units of $10^{-3} \text{ cm}^{-1} \text{ atm}^{-1}$. Estimated error bars (1σ) $\pm 0.5 \times 10^{-4} \text{ cm}^{-1} \text{ atm}^{-1}$.

$ m $	P branch	R branch
21	38.79	38.52
19	40.37	40.31
17	41.67	41.67
16	42.28	42.24
15	42.92	42.71
14	43.27	
13	43.72	43.64
11	44.64	44.61
9	45.87	45.84
8	46.96	46.65
7	48.05	47.92
6	49.65	
5	52.08	51.94
4	55.41	55.31
3	59.42	59.47
2	64.10	64.18
1	69.71	69.86

only for the mean kinetic energy $\langle E_k \rangle = 4kT/\pi$ (see below). The CO rovibrational energies were taken from the HITRAN database.²⁸

Before comparing theory and experiment, we first examine two aspects of the calculations. We begin with an examination of the importance of taking a thermal average. Most semiclassical calculations assume that an explicit average over E_k is not necessary and that the cross section may be determined by performing a single calculation at the kinetic energy corresponding to the mean relative velocity, i.e., at an energy equal to $4k_B T/\pi$. Using the known interaction potential for CO–He,²⁹ we have tested this approximation by performing full quantal calculations of the shifts of the pure rotational band, one by thermal averaging over energy and one at a single kinetic energy associated with the relative velocity. Figure 6(a) compares the two calculated shifts, $\delta^{0-0}(m>0)$. The results show that there is reasonable agreement for most of the values of m examined. For the case of CO–Ar, where the potential is not well known and given that the full calculations are time consuming, we use the above result to justify calculations only at the mean speed. For CO–He, where the potential is well known, the full calculations were done.

In the Introduction we implied that we would compare experimental results with quantal calculations but interpret the results using relationships between shifts that have only been established using a semiclassical theory. As an example, our second test justifies this assumption for one of the relationships. Once again, using the CO–He potential, we carry out a full quantal calculation of the shifts but now for the fundamental P and R branch. We wish to compare the shifts for the fundamental (vibrational) band to the shifts for the pure rotational band. As shown in the Appendix, using general properties of the semiclassical theory and with reasonable assumptions, the shifts, $\delta^{0-0}(m>0)$, $\delta^{0-1}(m>0)$, and $\delta^{0-1}(m<0)$ are related. The relationship is $\delta^{0-0}(m>0) = \delta_o^{0-1}(m>0)$, the latter being a quantity, odd in m , that we have defined earlier as $(1/2)[\delta^{0-1}(m) - \delta^{0-1}(-m)]$. Figure 6(b) shows that the relationship between $\delta^{0-0}(m>0)$ and

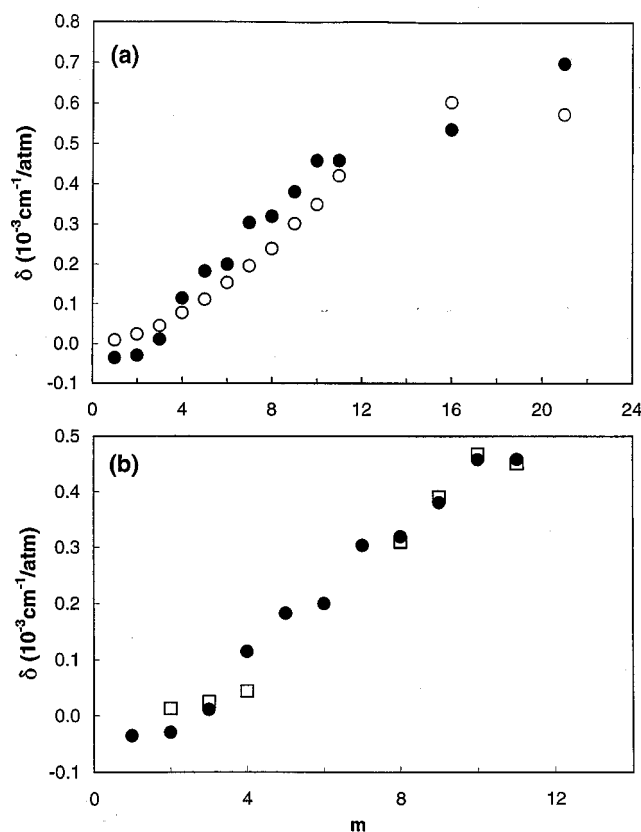


FIG. 6. Theoretical close coupled calculations of shifts for CO–He at $T = 296$ K. The solid points are the shifts for the pure rotational band, $\delta^{0-0}(m > 0)$, calculated over a full thermal average. In panel (a) these are compared with the same quantity but calculated using a mean relative speed (open circles) while in panel (b) they are compared with a few values (open square) of the full thermally average values of δ_o^{0-1} , the odd component of the shifts for the vibrational band.

$\delta_o^{0-1}(m > 0)$ is well obeyed by the full *quantal* calculation. We conclude that we will be justified in interpreting *any* quantitative disagreement between full quantal calculations in terms of qualitative relations derived on the basis of a *semiclassical* calculation. In particular we will take as shown, that the component of the shift, odd in m , is determined by the anisotropic component of the potential and that the even component of the shift is mostly determined by the vibrational dependence of the isotropic component of the interaction (see the Appendix). We are now in a position to comment upon the agreement or disagreement between the experimental values (points) of the broadening and shifting coefficients and the calculated values (solid lines), previously shown in Figs. 3–5.

VI. COMPARISON OF THEORY AND EXPERIMENT

A. Shifting in CO–He

In Fig. 3(b) we compare the present shifting measurements in CO–He with the thermally averaged quantal calculations of δ_e^{0-1} , that part of the shifts in the fundamental band of CO that is symmetric or even in the line number. In Fig. 3(c), we compare theoretical and experimental values of δ_o^{0-1} , that part of the shift that is antisymmetric or odd in line

number. We see that the experimental and theoretical values of δ_o^{0-1} are in excellent agreement. Based on the semiclassical theory we conclude that the anisotropic part of the CO–He potential, as given by Heijmen *et al.*,²⁹ is correct. (Note, in passing, if we had used the shifts of the first few R lines reported in Ref. 13 there would have been a significant disagreement between theory and experiment for these lines. This is a further indication that the present results are the more reliable for these lines.) From Fig. 3(b) we see that there is a factor of 2 disagreement between theory and experiment in the case of that part of the shifts that is even in line number. Therefore, we conclude that the vibrational dependence of the isotropic part of the potential for CO–He needs to be revised. Reid *et al.*³⁰ found a similar disagreement when comparing calculated and measured vibrationally inelastic cross sections. However, the present results alone cannot be used to revise the potential. The shifts from the short-range and the long-range interaction usually have opposite signs,³¹ so that the net shift is temperature dependent. It remains to be shown if shift measurements at different temperatures will be sufficient to determine the vibrational dependence of the isotropic part of the interaction potential.

B. Shifting in CO–Ar

The most precisely determined potential for CO–Ar is that of Toczyłowski *et al.*³² It contains the angular dependence but no vibrational dependence of the CO–Ar interaction. Nevertheless, we can still calculate δ_o^{0-1} , that part of the shift that is odd in m . As we saw in Fig. 6(b) for CO–He, δ_o^{0-1} is well approximated for $m > 0$ by δ^{0-0} , a quantity that depends only on the anisotropic part of the molecular interaction. (A semiclassical proof of equality of the two shifts is given in the Appendix.) We use this relationship for the CO–Ar, close coupled calculations. With the objective of reducing the computational time, we carry out the quantum close coupled calculations at only the mean relative kinetic energy, an approximation which was justified above. It is the value of $\delta^{0-0}(m > 0)$ calculated for CO–Ar (making both approximations) that is plotted in Fig. 4(c). The level of agreement between theory and experiment in Fig. 4(c) is exceptional. It is only for values of $|m|$ below 3 or 4 that the level of disagreement between theory and experiment may be significant. However, as noted above, we have probably underestimated the error bars for these broad lines and furthermore we cannot completely rule out the approximations made in the calculations as a source of small discrepancies between theory and experiment. Thus, we are not concerned about the small differences in Fig. 4(c). Finally, we remind the reader that the symmetric component of the shift may not be calculated without a knowledge of the vibrational dependence of the interaction and thus we cannot give a theoretical (solid) line in Figs. 4(a) or 4(b) for CO–Ar.

C. Broadening in CO–He

In Fig. 5(a) we see that the present measurements of the broadening coefficients, γ^{0-1} , at 296 K (solid points) are systematically higher than the values calculated for CO–He (solid line) by about 1%. This is well above the estimated

uncertainty of 0.1% in the experimental values. There are several possible sources of the discrepancy. Two of these are (i) the potential may be slightly in error; (ii) we may not be justified in ignoring the speed dependence of the broadening. When the relaxation rates are speed dependent, it is not correct to equate a thermally averaged relaxation rate to the width of a line.⁹ However, for atmospheric modeling or for establishing scaling laws, agreement at the 1% level is very satisfactory. In passing, we note that the calculations themselves have a numerical limit of accuracy but the lack of a smooth behavior that is apparent in plots of the calculated values versus line number is real and is probably associated with residual quantization effects and not with numerical errors (cf. Fig. 2 in Ref. 13, where significant “irregularities” with varying m are apparent).

D. Broadening in CO–Ar

The broadening, γ , depends both upon the vibrational and the orientational variation of the interaction potential (cf. Ref. 14 for a semiclassical justification of this statement). However, it is well known that CO broadening cross sections, in contrast to the shifting cross sections, depend only slightly on vibration¹⁴ and consequently are almost band independent. For the broadening in CO–Ar [Fig. 5(b)], we see that our close coupling results for the pure rotational band are in reasonable agreement with the observed values in the 0–1 band, although our calculations are 5% too large at very low values of $|m|$ and 2% too low for $|m| \geq 10$. Perhaps the small discrepancy can be attributed to the use of only a mean speed in the quantal calculations.

VII. SUMMARY AND CONCLUSIONS

In this paper we have presented experimental measurements of the shift in the P and R branch lines of the fundamental band of CO perturbed by He and Ar. We have compared these measurements and measurements of the broadening coefficients with full close coupled quantal calculations. We have shown that a decomposition of the shifts into components even (symmetric) and odd (antisymmetric) in the line number is beneficial to unraveling the contributions to the shifts of different parts of the interaction. It has long been a practice of theoreticians to test potential energy surfaces using thermodynamic data (PVT), transport coefficients, dimer spectra, etc. We have shown that shifts promise to be useful to the same end and in particular that the shifts symmetric in m may provide, along with inelastic vibrational cross sections, a sensitive test of the vibrational dependence of the interaction. For example, we have shown for CO–He that the vibrational dependence of the isotropic interaction needs to be revised. For CO–Ar we essentially confirmed the orientational part of the interaction potential. Overall we have shown, once the potentials are established, that close coupled quantal calculations are reliable and could be used to justify any empirical model of the temperature dependence of broadening and shifting, etc., of isolated lines. The calculations can be extended to simple diatom–diatom interactions.³³ However, from a practical point of view, we are still somewhat removed from being able to extend the

process to molecule–molecule interaction, for the more complex molecules that are relevant to atmospheric work.

ACKNOWLEDGMENTS

On the Canadian side, the authors would like to acknowledge the financial support of the Natural Sciences and Engineering Research Council of Canada, the Canadian Space Agency, the Atmospheric Environment Service, the Industrial Research Chair in Atmospheric Remote Sounding from Space, COMDEV, Bomem and the University of Toronto Research Fund.

APPENDIX

In this Appendix we prove, given reasonable approximations, that the P and R branch shifts contain a term, arising from the anisotropic interaction between the active diatomic molecule and a perturbing atom, that is antisymmetric or odd in m . For all semiclassical calculations, the shifting cross section at a temperature T is given by

$$\sigma_{fi}(T) = \int_0^\infty x e^x \sigma_{fi}(E) dx, \quad (\text{A1})$$

where $\sigma_{fi}(E)$ is given by

$$\begin{aligned} \sigma_{fi}(E) = & - \int_0^\infty 2\pi b db \\ & \times \sum_{m_i, m'_i, m_f, m'_f, q} (-1)^{m_f m'_f} \begin{pmatrix} j_i & 1 & j_f \\ m'_i & q & -m'_f \end{pmatrix} \\ & \times \begin{pmatrix} j_i & 1 & j_f \\ m_i & q & -m_f \end{pmatrix} \text{Im}[\Delta(E, b)]. \end{aligned} \quad (\text{A2})$$

Here, the fundamental quantity $\text{Im}[\Delta(E, b)]$ is a reduced shifting cross section. It is given in terms of matrix elements of the diffusion operator, S , by

$$\begin{aligned} \text{Im}[\Delta(E, b)] = & \text{Im}[\langle v_{ij} j_i m_i | S(b, E) | v_{ij} j_i m'_i \rangle \\ & \times \langle v_{fj} j_f m_f | S(b, E) | v_{fj} j_f m'_f \rangle]. \end{aligned} \quad (\text{A3})$$

If the atom–diatom potential is written as the sum $V(R, \theta, r) = V_i(R, r_e) + V'$, where $V_i(R, r_e)$ is the isotropic or spherically symmetric part of the potential at the equilibrium CO length, r_e , and V' is the rest, then $S(b, E)$ is a time-ordered series given by

$$S(b, E) = \exp \left[- (i/\hbar) \int_0^\infty \mathbf{V}'(t) dt \right], \quad (\text{A4})$$

where \mathbf{V}' is V' in the “interaction picture.” Writing the total potential as the sum of an isotropic and an anisotropic part, V' becomes $V' = \Delta V_i + V_a$, where $\Delta V_i = V_i(R, r) - V_i(R, r_e)$. The anisotropic part of the potential, V_a , may be expanded in Legendre polynomials as $V_a = \sum_l V_l(R, r) P_l(\cos \theta)$.

So far, we have outlined the general semiclassical theory of the shifts. We now make several simplifying assumptions. First, we assume that vibrationally inelastic processes may be ignored. Thus, only the elements of V' , diagonal in v ,

need be calculated, i.e., all we need calculated are $\langle v | \Delta V_i(R, r) | v \rangle$ and $\sum_l \langle v | V_l(R, r) | v \rangle P_l(\cos \theta)$. Next, we assume that the vibrational dependence of the anisotropic part of the potential is weak so that $\langle v | V_l | v \rangle$ becomes independent of v . If, in addition, we neglect vibration-rotation interaction we can evaluate it at the equilibrium position, r_e . Consequently V_a acts only on the rotational states $|J, m\rangle$. Of course, $\Delta V_i(R, r)$ acts only on the vibrational states $|v\rangle$ and not on $|J, m\rangle$. Collecting this all together allows us to write the quantity of interest, $\text{Im} \Delta(E, b)$, as

$$\text{Im}[\Delta(E, b)] = \text{Im}[e^{i\eta_v} \langle j_i m_i | S_a | j_i m_i' \rangle \langle j_f m_f | S_a | j_f m_f' \rangle]. \quad (\text{A5})$$

Here, the vibrational phase shift, η_v , arises from the isotropic part of the potential and is given by

$$\eta_i = \hbar^{-1} \int_{-\infty}^{\infty} [\langle v_f | \Delta V_i | v_f \rangle - \langle v_i | \Delta V_i | v_i \rangle] dt, \quad (\text{A6})$$

and the diffusion operator coming from the anisotropic part of the potential, S_a , is given by the time-ordered expression

$$S_a = \exp \left[-i\hbar \int_{-\infty}^{\infty} \mathbf{V}_a(t) dt \right]. \quad (\text{A7})$$

Both S_a and η_v are functions of b and E . We now assume that the vibrational phase shift is sufficiently small for significant values of b and E that we may write $\exp[-i\eta_v] \approx 1 - i\eta_v$. Thus, the fundamental quantity for the shifts, $\Delta(E, b)$, is given approximately by

$$\Delta(E, b) = \text{Im}[\langle j_i m_i | S_a | j_i m_i' \rangle \langle j_f m_f | S_a | j_f m_f' \rangle - \eta_v \text{Re}[\langle j_i m_i | S_a | j_i m_i' \rangle \langle j_f m_f | S_a | j_f m_f' \rangle]. \quad (\text{A8})$$

Next, we write the complex number $\langle j_i m_i | S_a | j_i m_i' \rangle$ as an amplitude times an exponential rotational phase shift, $\eta_r(j_i, m_i, m_i')$, arising from the anisotropic potential, i.e., $\langle j_i m_i | S_a | j_i m_i' \rangle = |\langle j_i m_i | S_a | j_i m_i' \rangle| \exp[i\eta_r(j_i)]$, with a corresponding expression for the final state. Thus, the shifts vary as $\text{Im}\{\exp[i\eta_r(j_i) - \eta_r(j_f)]\} - \eta_v \text{Re}\{\exp[i\eta_r(j_i) - \eta_r(j_f)]\}$, i.e., the shifts vary as $\{\sin[\eta_r(j_i) - \eta_r(j_f)] - \eta_v \cos[\eta_r(j_i) - \eta_r(j_f)]\}$.

We can now compare the shifts in the P and R branches for the same values of the line number. Or, which is the same, we compare the shift of the P($J+1$) line with the shift of the R(J) line. For R(J) we have $j_i = J$, $j_f = J+1$, and a net anisotropic phase shift of $[\eta_r(J) - \eta_r(J+1)]$. For P($J+1$) we have $j_i = J+1$, $j_f = J$, and a net anisotropic phase shift of $[\eta_r(J+1) - \eta_r(J)]$, the same in magnitude as for the R(J) line but opposite in sign. We have therefore shown that the shifts have a part, $\sin[\eta_r(j_i) - \eta_r(j_f)]$, arising only from the anisotropic interaction, which is odd in m . There is also a part of the shift, arising from both isotropic and anisotropic interactions, $\eta_v \cos[\eta_r(j_i) - \eta_r(j_f)]$, that is even in m . As an aside, note that one can claim that the pure vibrational phase shift, η_v , is partly "screened" by a term, $\cos[\eta_r(j_i) - \eta_r(j_f)]$, coming from the anisotropic part of the potential.

For the pure rotational band, $v_i = v_f$, and the vibrational phase is zero. It therefore follows from Eqs. (A2) to (A8) that the shifts of the pure rotational band vary as $\sin[\eta_r(j_i) - \eta_r(j_f)] = \sin[\eta_r(J) - \eta_r(J+1)]$. Thus, the shifts of the rotational lines are equal to the odd component of the shifts of the R lines of the vibrational band. In other words, the semi-classical theory, with reasonable approximations, predicts

$$\delta^{00}(m > 0) = \delta_o^{01} = \frac{1}{2} [\delta^{01}(m) - \delta^{01}(-m)]. \quad (\text{A9})$$

- ¹J. Bonamy, D. Robert, and C. Boulet, *J. Quant. Spectrosc. Radiat. Transf.* **31**, 23 (1984).
- ²A. Predoi-Cross, C. Luo, P. M. Sinclair, J. R. Drummond, and A. D. May, *J. Mol. Spectrosc.* **198**, 291 (1999).
- ³P. M. Sinclair, P. Duggan, R. Berman, J. R. Drummond, and A. D. May, *J. Mol. Spectrosc.* **191**, 258 (1998).
- ⁴R. Herman, *Phys. Rev.* **132**, 262 (1963).
- ⁵P. Joubert, M.-L. Dubernet, J. Bonamy, and D. Robert, *J. Chem. Phys.* **107**, 3845 (1997).
- ⁶P. Duggan, P. M. Sinclair, M. P. Le Flohic, J. W. Forsman, R. Berman, A. D. May, and J. R. Drummond, *Phys. Rev. A* **48**, 2077 (1993).
- ⁷C. Luo, R. Berman, A. Predoi-Cross, J. R. Drummond, and A. D. May, *J. Mol. Spectrosc.* **196**, 290 (1999).
- ⁸P. W. Rosenkranz, *IEEE Trans. Antennas Propag.* **AP-23**, 498 (1975).
- ⁹A. D. May, *Phys. Rev. A* **59**, 3495 (1999).
- ¹⁰S. H. Fakhri-Eslam, G. D. Sheldon, J. R. Drummond, and A. D. May, *J. Quant. Spectrosc. Radiat. Transf.* **68**, 377 (2001).
- ¹¹R. L. Farrow, L. A. Rahn, and G. O. Sitz, *Phys. Rev. Lett.* **63**, 746 (1989).
- ¹²A. J. Mannucci, *J. Chem. Phys.* **95**, 7795 (1991).
- ¹³F. Thibault, J. Boissoles, R. Le Doucen, R. Farrenq, M. Morillon-Chapey, and C. Boulet, *J. Chem. Phys.* **97**, 4623 (1992).
- ¹⁴J. P. Bouanich, F. Rachet, and A. Valentin, *J. Mol. Spectrosc.* **178**, 157 (1996).
- ¹⁵N. Anselm, K. M. T. Yamada, R. Schieder, and G. Winnewisser, *J. Mol. Spectrosc.* **161**, 284 (1993).
- ¹⁶B. Sumpf, J. P. Burrows, A. Kissel, H. D. Kronfeldt, O. Kurtz, I. Meusel, J. Orphal, and S. Voigt, *J. Mol. Spectrosc.* **190**, 226 (1998).
- ¹⁷T. Drascher, T. F. Giesen, T. Y. Yang, N. Schmucker, R. Schieder, G. Winnewisser, P. Joubert, and J. Bonamy, *J. Mol. Spectrosc.* **192**, 268 (1998).
- ¹⁸A. Ben Reuven, *Phys. Rev.* **145**, 7 (1966).
- ¹⁹R. Shafer and R. G. Gordon, *J. Chem. Phys.* **58**, 5422 (1973).
- ²⁰J. M. Hutson, and S. Green, MOLSCAT, version 14, distributed by Collaborative Computational Project 6 (Daresbury Laboratory UK Engineering and Physical Sciences Research Council), 1995.
- ²¹A. M. Arthurs and A. Delgarno, *Proc. R. Soc. London, Ser. A* **256**, 540 (1960).
- ²²D. R. Fowler, D. Bourhis, and J. M. Launay, *Comput. Phys. Commun.* **131**, 187 (2000).
- ²³R. T. Pack, *J. Chem. Phys.* **60**, 633 (1974).
- ²⁴A. Omont, *Prog. Quantum Electron.* **5**, 69 (1977).
- ²⁵P. Bréchnignac, A. Picard-Bersellini, R. Charneau, and J. M. Launay, *Chem. Phys.* **53**, 165 (1980).
- ²⁶F. Thibault, B. Calil, J. Boisseles, and J. M. Launay, *Phys. Chem. Chem. Phys.* **2**, 5404 (2000).
- ²⁷B. R. Johnson, *J. Chem. Phys.* **69**, 4678 (1978).
- ²⁸L. S. Rothman, C. P. Rinsland, A. Goldman *et al.*, *J. Quant. Spectrosc. Radiat. Transf.* **60**, 665 (1998).
- ²⁹T. G. A. Heijmen, R. Mosynski, P. E. S. Wormer, and Ad der Averoid, *J. Chem. Phys.* **107**, 9921 (1997).
- ³⁰J. P. Reid, C. J. S. Simpson, and H. M. Quiney, *J. Chem. Phys.* **107**, 9929 (1997).
- ³¹A. D. May, G. Varghese, J. C. Stryland, and H. L. Welsh, *Can. J. Phys.* **42**, 1058 (1964).
- ³²R. R. Toczykowski and S. M. Cybulski, *J. Chem. Phys.* **112**, 4604 (2000).
- ³³W. M. Huo and S. Green, *J. Chem. Phys.* **104**, 7572 (1996).